Experimental characterization and numerical lifetime prediction of adhesively bonded joints under multiaxial fatigue loading

S. Çavdar[1], G. Meschut[1], U. Kroll[2], A. Matzenmiller[2]
[1]Laboratory for Materials and Joining Technology (LWF), Paderborn University
[2]Institute of Mechanics (IfM), University of Kassel
serkan.cavdar@lwf.upb.de

Introduction

Adhesive joining technologies are particularly used in bodyshell constructions to apply innovative lightweight designs for the reduction of fuel consumption and CO_2 emissions. A reliable lifetime prediction is of great importance for the dimensioning of adhesive bonds, which are subjected to cyclic and multiaxial local stress fields as a result of time-dependent external loadings.
Out of this motivation, a concept is presented, based on experimental characterization in [1] and constitutive modeling in [2, 3], for the lifetime prediction of structural adhesives. Creep and fatigue damage evolution due to static and cyclic loading are modeled with a differential equation, based on continuum damage mechanics. Two equivalent stresses take multiaxial creep and fatigue failure into consideration. For the parameter identification, uni- and multiaxial creep and fatigue tests are performed with the butt-bonded double hollow cylinder (DHC) specimen. The model implementation into the finite element software LS-DYNA as a user material and the identified parameters are validated by means of cyclic tests of the L-specimen.

Experimental investigations

The DHC specimen with the dimensions in Figure 1 consists of two steel tubes with a wall thickness of 3 mm in the bonding area. The tubes are made from the adherend material S235 JRG2+C and are butt-bonded with a toughened epoxy-based structural adhesive (Dow BETAMATE™ 1496 V) with a layer thickness of t_a = 0.3 mm. The adhesive surfaces are sand blasted and pretreated with an adhesion promoter (DELO-SACO® PLUS). After curing of the adhesive in a convection oven at a temperature of 180 °C over 30 min, the specimen is stored at a temperature of 23 °C and a relative humidity of 50% for at least 10 days. During the test, the specimen suffers axial F and torsional loading M_T implying nearly homogeneous tension σ and shear τ in the bonding layer:

$$\sigma = \frac{4}{\pi\left(d_a{}^2 - d_i{}^2\right)} \cdot F \quad , \quad \tau = \frac{16 \cdot d_a}{\pi \cdot \left(d_a{}^4 - d_i{}^4\right)} \cdot M_T \qquad (1)$$

For the characterization of the fatigue behavior, load controlled uni- and multiaxial fatigue tests with load ratio $R = \sigma_{min}/\sigma_{max} = 0.1$ and frequency $f = 10$ Hz at constant shear-tensile stress amplitude ratios τ_a/σ_a of ∞, 0, 0.5 and 2 are performed with 10^3 to 10^6 cycles N_f until complete failure of the adhesive joint. The resulting S-N test data are illustrated in Figure 4. A more detailed description of the production process of the DHC specimen, the test setup and corresponding results are given in [1].

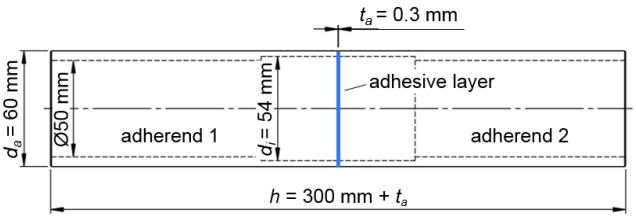

Figure 1. Dimensions of butt-bonded double hollow cylinder (DHC) specimen.

Besides the fatigue tests, uni- and multiaxial creep tests with shear-tension ratios τ/σ of ∞, 0, 0.5 and 2 and creep rupture times t_R between 1 h and 10^3 h are performed, resulting in the test data in Figure 5.
For the model validation, the so-called L-specimen with the dimensions in Figure 2 is developed consisting of steel sheets from HC340LA+ZE75/75 with a thickness of 1.5 mm and an adhesive layer thickness of 0.3 mm. The L-specimen represents a combination of single-lap shear (DIN EN 1465) and T-peel specimen (DIN EN ISO 11339) and permits multiaxial load initiation with inhomogeneous stress fields in the adhesive layer. In contrast to the DHC specimen, the adhesive surfaces are degreased. The curing procedure is similar to the DHC specimen.
Based on quasistatic investigations, multiaxial fatigue tests are performed with in-phase loadings $F_1(t)$ and $F_2(t)$ having constant amplitudes over time t, $f = 10$ Hz and load ratio $R_F = F_{min}/F_{max} = 0.1$ until fracture. The experimental results are shown in Figure 7.

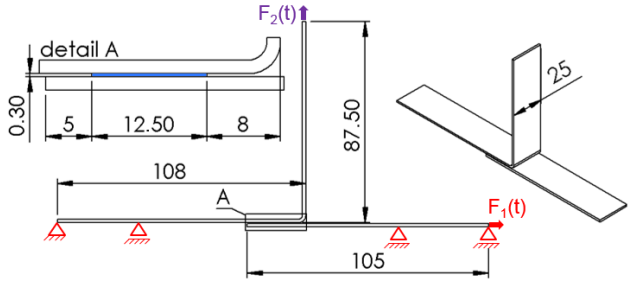

Figure 2. Dimensions and loading of the L-specimen.

Modeling and parameter identification

The thin adhesive joint is idealized as a linear viscoelastic interface, which constitutive behavior in effective stresses is described by the convolution integral

$$\begin{bmatrix} \tilde{t}_t \\ \tilde{t}_b \\ \tilde{t}_n \end{bmatrix} = \int_0^t \begin{bmatrix} R_s(t-\tau) & 0 & 0 \\ 0 & R_s(t-\tau) & 0 \\ 0 & 0 & R_n(t-\tau) \end{bmatrix} \frac{d}{d\tau} \begin{bmatrix} \Delta_t \\ \Delta_b \\ \Delta_n \end{bmatrix} d\tau \qquad (2)$$

relating the effective traction vector $\tilde{t}_i = [\tilde{t}_t \quad \tilde{t}_b \quad \tilde{t}_n]^T$ to the displacement jump vector $\Delta_i = [\Delta_t \quad \Delta_b \quad \Delta_n]^T$. The re-

laxation functions R_s and R_n depend on time t and consist of PRONY-series with interface stiffnesses k_{si} and k_{ni} and relaxation times $\hat{\tau}_{si}$ and $\hat{\tau}_{ni}$ for shear and normal direction:

$$R_s(t-\tau) = \sum_{i=1}^{N} k_{si} \exp\left(-\frac{t-\tau}{\hat{\tau}_{si}}\right) \quad (3)$$

$$R_n(t-\tau) = \sum_{i=1}^{N} k_{ni} \exp\left(-\frac{t-\tau}{\hat{\tau}_{ni}}\right) \quad (4)$$

The identification of the viscoelastic parameters for $N = 2$ is described in [3] and results in the values in Table 1.

The effective traction vector $\tilde{t}_i$ is related to the actual tractions vector t_i according to the effective stress concept by

$$t_i = (1-D)\tilde{t}_i \quad (5)$$

The proposed model for the evolution of damage D is a nonlinear first order ordinary differential equation, which consists of the creep $\dot{D}_c$ and fatigue damage part $\dot{D}_f$:

$$\dot{D} = \underbrace{\frac{1}{c_0}\left(\frac{\langle \sigma_{eqc} - \sigma_{dc} \rangle}{\sigma_{ref}(1-D)}\right)^n}_{\dot{D}_c} + \underbrace{\left(\frac{\langle \sigma_{eqf} - \sigma_{df} \rangle}{(\sigma_u - \sigma_{df})(1-D)}\right)^k \frac{\langle \dot{\sigma}_{eqf} \rangle}{\sigma_u - \sigma_{df}}}_{\dot{D}_f} \quad (6)$$

Equation (6) contains three parameters σ_{dc}, σ_{ref}, and n in the creep and three parameters σ_{df}, σ_u and k in the fatigue damage part. The variable $c_0 = 1$ s ensures consistent units and $\langle x \rangle = (x + |x|)/2$ is the MACAULAY operator. The test data of the DHC specimen in Figures 4 and 5 do not allow the identification of the creep σ_{dc} and fatigue durability σ_{df}, which is why they are set to zero. For positive cyclic tractions, the equivalent stresses σ_{eqc} and σ_{eqf} of the interface for creep and fatigue are given by

$$\sigma_{eqc} = \sqrt{b_{1c} t_n^2 + b_{2c} t_n + t_t^2 + t_b^2} \quad (7)$$

$$\sigma_{eqf} = \sqrt{b_{1f} t_n^2 + b_{2f} t_n + t_t^2 + t_b^2} \quad (8)$$

The parameters b_{1c}, b_{2c} and b_{1f}, b_{2f} in the equivalent stresses σ_{eqc} and σ_{eqf} take multiaxial creep and fatigue loading into account by the consideration of the influence of the normal traction t_n.

All parameters in equations (6) to (8) are identified by means of the test data in Figures 4 and 5. For the identification of n and σ_{ref}, pure shear creep loading

$$\sigma_{eqc} = \sigma_{eqf} = t_t = t_{tm} = \text{const.} > \sigma_{dc}\,,\ t_n = t_b = 0 \quad (9)$$

is inserted in equation (6), which is integrated from $D = 0$ at $t = 0$ to $D = 1$ at rupture time $t = t_R$ resulting in the double logarithmic straight line

$$\log(t_{tm} - \sigma_{dc}) = -\frac{1}{n}\log\frac{t_R}{c_0} + \log\left(\frac{\sigma_{ref}}{(n+1)^{\frac{1}{n}}}\right) \quad (10)$$

The parameters n and σ_{ref} determine the vertical intercept, while only the parameter n influences the slope. Thus, the creep damage parameters σ_{dc}, σ_{ref}, and n are analytically identified by means of creep tests until rupture.

The meaning of the fatigue damage parameters σ_u and k is apparent, when creep damage is neglected, i. e. $D_c = 0$, $D = D_f$. Then, inserting positive pure shear fatigue loading

$$\sigma_{eqc} = \sigma_{eqf} = t_t = t_{tm} + t_{ta}\sin(2\pi f t) > 0\,,\ t_n = t_b = 0 \quad (11)$$

in equation (6) allows integration from $D = 0$ at $N = 0$ to $D = 1$ at the number of cycles to failure $N = N_f$ resulting in the double logarithmic straight line

$$\log t_{ta} = -\frac{1}{k+1}\log N_f + \log\left(\frac{\sigma_u(1-R)}{2\sqrt[k+1]{1-R^{k+1}}}\right) \quad (12)$$

Here, the parameters σ_u and k determine the vertical intercept and the slope. Because of the simplifying assumption $D_c = 0$, the analytically determined parameters σ_u and k by equation (12) are optimized with the software LS-OPT. Hence, the lifetimes computed by numerical solutions of equation (6), which is described in [2] in detail, are fitted to the test data in the case of pure shear fatigue loading (11), whereby the previously identified parameters n and σ_{ref} are applied.

After the identification of the parameters n, σ_{ref}, σ_u and k, the parameters b_{1c}, b_{2c} and b_{1f}, b_{2f} are determined by fitting the numerically predicted lifetimes due to uni- and multiaxial creep and fatigue loadings with tension to the corresponding test data. The resulting values of the parameter identification are listed in Table 2.

Table 1. Viscoelastic parameters [2, 3].

k_{s1} [MPa/mm]	k_{s2} [MPa/mm]	$\hat{\tau}_{s1}$ [s]	$\hat{\tau}_{s2}$ [s]
461.2	329	5782.2	250249.6
k_{n1} [MPa/mm]	k_{n2} [MPa/mm]	$\hat{\tau}_{n1}$ [s]	$\hat{\tau}_{n2}$ [s]
2425	916	11197	368762

Table 2. Parameters for damage approach [2].

σ_{dc} [MPa]	σ_{ref} [MPa]	n [-]	b_{1c} [-]	b_{2c} [MPa]
0	51	19	0.5	12
σ_{df} [MPa]	σ_u [MPa]	k [-]	b_{1f} [-]	b_{2f} [MPa]
0	49	19	0.4	21

Verification

The numerical solution of the model equations (2) to (8) is implemented in [2] as a user defined material into the FE-program LS-DYNA. A cycle jump and a multiscale method, both described in detail in [2], are implemented for the reduction of the computation times of the analyses with cyclic loadings, for which a cycle is discretized with 16 time steps per period. The time step size for the creep loadings is 10 seconds.

The implementation is verified by means of numerical lifetime predictions for the DHC specimen with LS-DYNA due to implicit FE-analyses. Therefore, the FE-model in Figure 3 is created with LS-Prepost. Only the adhesive layer and its surrounding area of the steel tubes are modeled with 32 elements in direction of the circumference. The adhesive is modeled with cohesive zone elements with

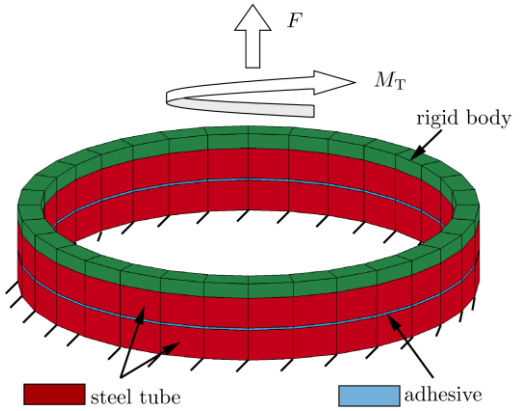

Figure 3. FE-model of the DHC specimen.

one element over the layer thickness. Linear solid elements with linear elastic material behavior of ordinary steel are used for the tubes. The loading with axial force F and moment M_T is applied with a rigid body. The nodes of the steel tube on the opposite side of the rigid body are fixed. The force controlled FE-analyses are fully implicit with full newton method and standard values of LS-DYNA. The computation terminates after every interface element is deleted due to total damage $D = 1$ at all their gauss points. The comparison of test data and lifetime predictions in logarithmic scales in Figures 4 and 5 for fatigue and creep fracture of the adhesive joint verify the implementation. In Figure 5, the prediction of the rupture time due to the normal stress component σ for τ/σ=2 is not a straight line, which results from the approach for the equivalent stress.

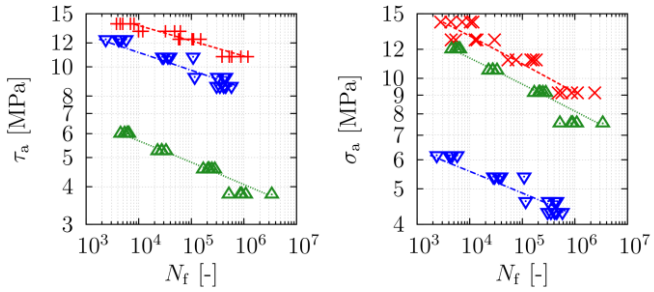

Figure 4. Comparison of fatigue test data for $\tau_a/\sigma_a=\infty$ (+), 0 (X), 0.5 (Δ) and 2 (∇) with predictions (lines) for the DHC.

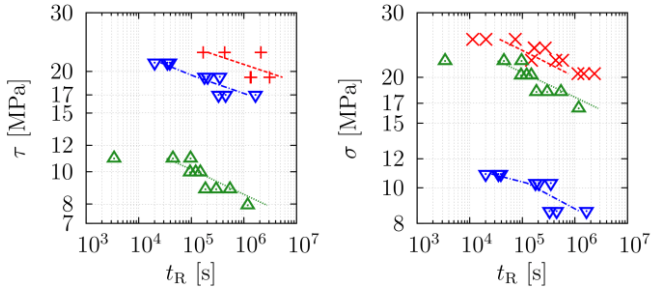

Figure 5. Comparison of creep test data for τ/σ=∞ (+), 0 (X), 0.5 (Δ) and 2 (∇) with predictions (lines) for the DHC.

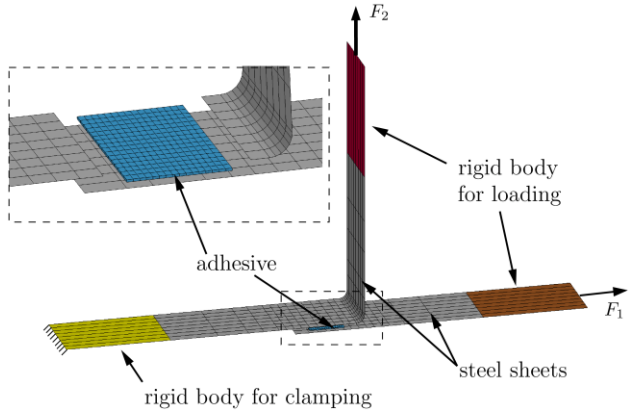

Figure 6. FE-model of the L-specimen.

Validation

The FE-model of the L-specimen in Figure 6 for the validation consists of a fixed rigid body representing the clamping and two rigid bodies for the load application. The adhesive layer is discretized with 16x16 cohesive elements. A so-called offset tied contact is used to connect the adhesive layer with the steel sheets modeled with 312 underintegrated shell elements and elastoplastic material behavior. Hourglass control is used in addition to the same settings for the implicit simulations of the DHC specimen. The implementation is successfully validated, see Figure 7. The predictions of the lifetimes until fracture are conservative in the case of loading considered in the left diagram, but are non-conservative in the right diagram: The deviations increase with increasing lifetime of the L-specimen.

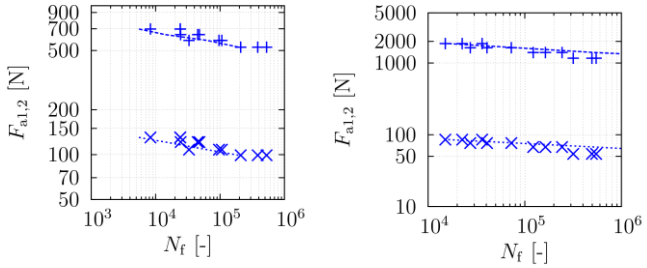

Figure 7. Test data and predictions (lines) for the L-specimen: Amplitudes of forces F_1 (+) and F_2 (X) over number of cycles to fracture.

Conclusions

The concept consisting of the experimental characterization for the parameter identification and the numerical lifetime prediction for the structural adhesive at hand is successfully validated. Only proportional cyclic loadings with constant amplitudes and load ratio $R = 0.1$ are considered. Thus, mean stress influence, variable amplitudes and non-proportional loadings have to be taken into account in forthcoming investigations.

Acknowledgements

Shown research results are taken from IGF research project 18107 N by research association for steel application FOSTA, which has been founded by the AiF under the program for promotion of industrial research (IGF) by the Federal Ministry of Economics and Energy based on a decision of the German Bundestag.

References

1. S. Çavdar, D. Teutenberg, G. Meschut, The Adhesion Society, *Proceedings of the 40th Annual Meeting*,2017.
2. U. Kroll, A. Matzenmiller: Fatigue strength evaluation of multiaxially loaded adhesively bonded steel joints. IGF research project 18107 N. FOSTA-Report P1028 (Sohnstr. 65, 40237 Düsseldorf), 215–350, in press.
3. A. Matzenmiller, B. Kurnatowski: Design of adhesive joints with steel components at loading with variable amplitudes for vehicle construction. IGF research project 307 ZN. M. Brede and F.-J. Heise (eds.), FOSTA-Report P796 (Verlag und Vertriebsgesellschaft mbH, Sohnstr. 65, 40237 Düsseldorf, 2012), 51–101, 133–138, 210–215.